



HAL
open science

Thermoresponsive nanogels based on polyelectrolyte complexes between polycations and functionalized hyaluronic acid

Huu van Le, Virginie Dulong, Luc Picton, Lecerf Didier

► **To cite this version:**

Huu van Le, Virginie Dulong, Luc Picton, Lecerf Didier. Thermoresponsive nanogels based on polyelectrolyte complexes between polycations and functionalized hyaluronic acid. *Carbohydrate Polymers*, 2022, pp.119711. 10.1016/j.carbpol.2022.119711 . hal-03692142

HAL Id: hal-03692142

<https://hal.science/hal-03692142>

Submitted on 22 Jul 2024

HAL is a multi-disciplinary open access archive for the deposit and dissemination of scientific research documents, whether they are published or not. The documents may come from teaching and research institutions in France or abroad, or from public or private research centers.

L'archive ouverte pluridisciplinaire **HAL**, est destinée au dépôt et à la diffusion de documents scientifiques de niveau recherche, publiés ou non, émanant des établissements d'enseignement et de recherche français ou étrangers, des laboratoires publics ou privés.



Distributed under a Creative Commons Attribution - NonCommercial 4.0 International License

1 **Thermoresponsive nanogels based on polyelectrolyte complexes**
2 **between polycations and functionalized hyaluronic acid**

3

4

5

6

7 Huu Van LE, Virginie DULONG, Luc PICTON, Didier LE CERF *

8 *Normandie Univ, UNIROUEN, INSA Rouen, CNRS, PBS UMR 6270, 76000 Rouen, France*

9

10

11

12

13

14

15

16 *Corresponding author: E-mail address: didier.lecerf@univ-rouen.fr

17 Tel: 00 33 02 35 14 65 43; Fax: 00 33 02 35 14 67 04

18 **ABSTRACT**

19 A novel kind of thermoresponsive polyelectrolyte complex-based nanogels (PEC-NGs) was
20 elaborated by mixing hyaluronic acid (HA) functionalized with Jeffamine® M-2005 (M2005, a
21 thermoresponsive amine-terminated polyether) and diethylaminoethyl dextran (DEAE-D) or
22 poly-L-lysine (PLL) in water. The presence of M2005 grafts led to PEC-NGs with larger particle
23 size, lower net surface charge and thermoresponsiveness, namely shrinkage with increasing
24 hydrophobicity at higher temperature. Both M2005 grafts and replacing DEAE-D with PLL as
25 polycation allowed PEC-NGs to have higher stability against salinity and better encapsulation of
26 curcumin, most probably through intraparticle hydrophobic interactions, whereas interparticle
27 hydrophobic interactions may facilitate particle aggregation over time. Curcumin encapsulation
28 can be optimized by applying higher temperature during the complexation. Enzymatic
29 degradability of PEC-NGs was also verified through particle size evolution in the presence of
30 hyaluronidase. These results provide new insights into the physicochemical aspect of such
31 systems as promising nanocarriers for drug delivery.

32

33 **Keywords:** nanogels; polyelectrolyte complexes; thermoresponsive; hyaluronic acid; Jeffamine®
34 M-2005

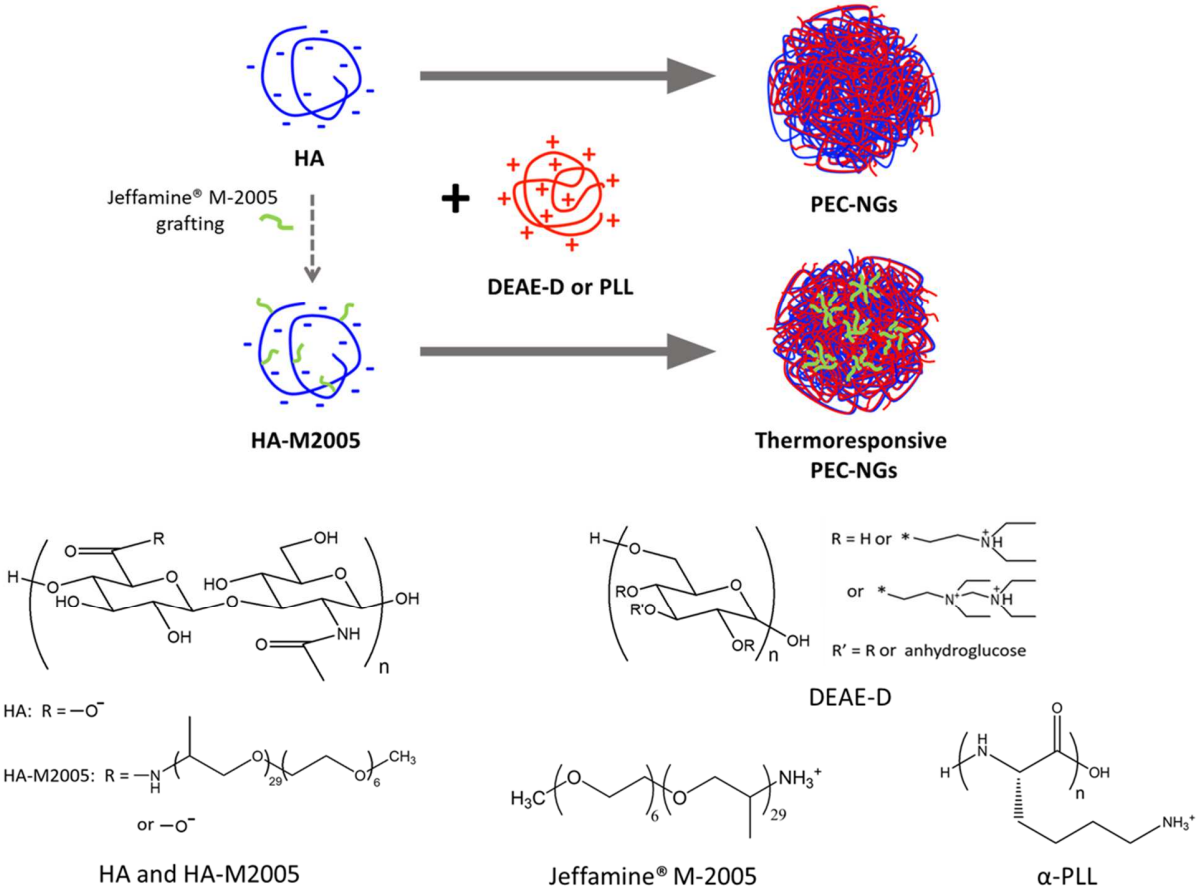
35 1. INTRODUCTION

36 Nanogels (NGs) based on polyelectrolyte complexes (PECs) can be formed spontaneously
37 through ion pairing between polyanions and polycations upon simple mixing in aqueous media
38 (Bonaccorso et al., 2021). Particularly, PEC-based NGs (PEC-NGs) from polysaccharides have
39 attracted a great deal of interest as drug delivery systems (DDS) due to their biocompatibility and
40 simple preparation requiring neither high energy nor organic solvents (Debele, Mekuria, & Tsai,
41 2016).

42 Thermoresponsive nanocarriers have received increasing attention as robust DDS (Bordat,
43 Boissenot, Nicolas, & Tsapis, 2019). They can be elaborated from thermoresponsive copolymers,
44 which display a temperature-dependent hydrophilic-hydrophobic balance due to difference in
45 solvation status between component monomers at different temperatures (Bordat et al., 2019;
46 Gandhi, Paul, Sen, & Sen, 2015). Among them, polymers disposing lower critical solution
47 temperature (LCST), which are water-soluble below a critical temperature but become insoluble
48 at a higher temperature due to higher hydrophobicity, have been extensively studied and
49 employed in DDS (Karimi et al., 2016). Nanoparticles from these polymers can show shrinkage
50 along with higher hydrophobicity at higher temperature, leading to applications in either
51 triggered-release or sustained-release of drugs (Karimi et al., 2016; Kim et al., 2019).
52 Accordingly, employing thermoresponsive derivatives of polysaccharides (i.e. polysaccharides
53 grafted with suitable LCST groups) in DDS has also become an emerging topic of research since
54 they can improve the encapsulation and release of hydrophobic drugs while conserving the
55 advantages of precursor biopolymers (Graham, Marina, & Blencowe, 2019).

56 From such perspectives, systems combining both the abovementioned aspects, i.e. PEC-NGs
57 from thermoresponsive polysaccharide derivatives, would be of high interest as DDS, yet have

58 not been reported in the literature to the best of our knowledge. In this context, our work aimed
 59 to elaborate and characterize such a novel kind of DDS from readily available materials, namely
 60 HA-M2005 which is hyaluronic acid (HA) functionalized with Jeffamine® M-2005 (M2005)
 61 and diethylaminoethyl dextran (DEAE-D) or poly-L-lysine (PLL) (**Figure 1**).



62
 63 **Figure 1.** Scheme of PEC-NG formation from polyanions (blue) (HA: hyaluronic acid or HA-
 64 M2005: hyaluronic acid functionalized with Jeffamine® M-2005 (green)) electrostatically
 65 complexed with polycations (red) (DEAE-D: diethylaminoethyl dextran or PLL: poly-L-lysine)
 66 and their chemical structures.

67 HA is an anionic polysaccharide extensively employed in DDS development due to its excellent
68 biocompatibility and biodegradability (Necas, Bartosikova, Brauner, & Kolar, 2008). CD44
69 receptors, which are natural receptors of HA, and hyaluronidase (HAase), which is a family of
70 enzymes catalyzing HA degradation, are both overexpressed in many cancer cells, e.g. in breast
71 and brain tumors (Stern, 2008; Xu, Niu, Yuan, Wu, & Liu, 2020). This renders HA-based nano-
72 DDS particularly interesting for drug targeting since they can be specifically uptaken and
73 degraded to release drugs inside these cells (Yang, Zhang, Chen, Chen, & Liu, 2016). M2005 is a
74 commercial diblock copolyether monoamine made up of amine-terminated poly(propylene
75 oxide) (PPO) and poly(ethylene oxide) (PEO), constituting a thermoresponsive copolymer with
76 LCST temperature of 14-30 °C (Agut, Brûlet, Taton, & Lecommandoux, 2007; Dulong, Mocanu,
77 Picton, & Le Cerf, 2012; Niang et al., 2016). In our previous work, M2005 was successfully
78 grafted on HA to obtain HA-M2005 as a thermoresponsive HA derivative with a sol-gel
79 transition depending on temperature (Madau, Le Cerf, Dulong, & Picton, 2021). DEAE-D is a
80 polycation with cationic DEAE groups grafted on dextran, a natural polysaccharide extracted
81 from plants or microbial fermentations (Díaz-Montes, 2021; Gulick, 1997). It is mainly used as
82 means for nucleic acids transfection or proteins delivery with good biocompatibility and high
83 solubility (Gulick, 1997; Huguet, Neufeld, & Dellacherie, 1996; Manosroi & Manosroi, 1997).
84 PLL is a biocompatible and biodegradable cationic polyaminoacid, which is largely used as
85 coating agent for cell adhesion promotion (Huguet et al., 1996). PLL coating can also increase
86 cell uptake of nanoparticles, which would improve therapeutic efficacy in targeted nanomedicine
87 (Siow et al., 2018).

88 Previously, our work has shown that mixing of HA and DEAE-D solutions can lead to formation
89 of HA/DEAE-D PEC-NGs having mean size of 150-350 nm with relatively hydrophobic cores

90 surrounded by hydrophilic corona shells of polar uncomplexed polyelectrolyte segments (Le,
91 Dulong, Picton, & Le Cerf, 2021). They can have good shelf stability in water but generally poor
92 stability against salt and slight hydrophobicity (Le et al., 2021). Our hypothesis is that PEC-NGs
93 prepared with HA-M2005 should present more interesting properties, such as dual-
94 responsiveness (thermoreponsiveness beside enzymatic-induced degradation), than with non-
95 modified HA. In this work, the effects of M2005 grafts and polycation structure on HA-based
96 PEC-NGs were elucidated after their preparation and characterization in terms of morphology,
97 particle size, zeta potential (ζ) and hydrophobicity with varying parameters, including constituent
98 polymers (**Figure 1**), temperature, salinity and storage time. Encapsulation of curcumin as a
99 model drug was realized to evaluate the potential of these systems as nanocarriers for delivering
100 poorly water-soluble drugs. Enzymatic degradation of such PEC-NGs was also investigated and
101 confirmed by observing particle size in the presence of HAase.

102 **2. MATERIALS AND METHODS**

103 **2.1. Materials**

104 HA and Jeffamine® M-2005 were kindly provided by Givaudan (France) and Huntsman (USA)
105 respectively. DEAE-D hydrochloride and α -PLL hydrobromide were purchased from Sigma-
106 Aldrich (USA). HA-M2005 was obtained by grafting Jeffamine® M-2005 to HA (degree of
107 substitution of 3.6 %) through EDC/NHS coupling reaction (Supplementary Information **SI-1**) as
108 reported in our earlier study (Madau et al., 2021).

109 **Table 1** summarizes macromolecular characteristics of the polyelectrolytes (Supplementary
 110 Information **SI-2**), with those of HA and DEAE-D retrieved from our previous work (Le et al.,
 111 2021). Pyrene was purchased from Acros Organics (USA). Curcumin, phosphate-buffered saline
 112 (PBS) tablets and HAase from sheep testes (400 IU.mg⁻¹) were purchased from Sigma-Aldrich
 113 (USA). Water purified by Milli-Q system (Millipore, USA) was used for all experiments.

114 **Table 1.** Characteristics of polyelectrolytes

Polyelectrolyte	M _n (g.mol ⁻¹)	M _w (g.mol ⁻¹)	Đ
HA	210,000	270,000	1.3
DEAE-D	270,000	700,000	2.6
PLL	200,000	490,000	2.5
HA-M2005	180,000	240,000	1.3

M_n: number average molecular weight; M_w: weight average molecular weight; Đ: dispersity

115 **2.2. Preparation of PEC-NGs**

116 PEC-NGs were prepared following the same method as our previous work (Le et al., 2021).
 117 Polyelectrolyte solutions at defined total polymer concentrations (C_p, excluding counterions)
 118 were prepared beforehand by dissolving polyelectrolytes in Milli-Q water under stirring
 119 overnight at room temperature and afterwards filtered through regenerated cellulose 0.45 μm
 120 membrane filter units (Sartorius, Germany). Each PEC-NG suspension at a definite C_p and n-/n+
 121 (molar ratio of negative to positive charges on component polyelectrolytes) was obtained by one-
 122 shot addition of polyanion to polycation solutions of the same C_p with the volume ratio deduced
 123 from n-/n+ (Supplementary Information **SI-3**), followed by 30 min of stirring at room
 124 temperature. At least three batches were prepared for each formulation.

125 For preparing curcumin-loaded NGs, before polycation addition, there was an additional step of
 126 dropping an amount of curcumin 5 g.L⁻¹ stock solution in acetone to the polyanion solution. The

127 ratio of curcumin to polyelectrolytes was fixed at 2/5 m/m. After 30 min of stirring at studied
128 temperatures (25 °C, 50 °C or 70 °C), all samples were left at room temperature over 12 h for
129 acetone evaporation. The precipitated non-encapsulated curcumin was then removed by
130 centrifugation at $3,000\times g$ for 15 min and the supernatant was filtered through polyvinylidene
131 difluoride (PVDF) 0.45 μm membrane filter units (Millipore, Germany) to obtain the filtrate as
132 PEC-NG suspension. Samples without polymers were also prepared as reference. All samples
133 were protected from light to avoid curcumin degradation.

134 **2.3. Particle size, zeta potential (ζ) and morphology analyses**

135 Particle size and ζ were characterized only for visually homogeneous NG suspensions without
136 further dilution using Zetasizer Ultra (Malvern Panalytical, UK). Mean hydrodynamic diameter
137 (D_h) and polydispersity index (PDI) were determined by dynamic light scattering (DLS) with
138 back-scatter mode. ζ was measured by electrophoretic light scattering. Every sample was
139 measured at least in triplicate after stabilization for 120 s at 25 °C or 300 s at 37 °C or 50 °C.

140 The morphologies of PEC-NGs were examined using a transmission electron microscope (TEM)
141 FEI Tecnai 12 BioTwin (Philips, The Netherlands) operating at 80 kV. For specimen
142 preparation, 10 μL of a PEC-NG suspension was placed on a formvar and carbon coated copper
143 grid for 15 min for adhesion of PEC-NGs on the grid and the excess suspension was then
144 removed by filter paper. 10 μL of phosphotungstic acid 1% solution was thereafter deposited on
145 the grid for contrast enhancement and wicked away after 30 s, followed by air-drying of the grid
146 before observation.

147 **2.4. Pyrene fluorescence**

148 Samples for pyrene fluorescence analyses were prepared as previously described (Le et al.,
149 2021). 1 mL of pyrene 8×10^{-7} mol.L⁻¹ aqueous solution was mixed with an equal volume of
150 PEC-NG suspensions ($C_P = 0.5$ g.L⁻¹) under stirring overnight. Fluorescence emission spectra of
151 samples upon excitation at 335 nm wavelength were recorded at certain temperatures (25 °C, 37
152 °C or 50 °C) using a Fluoromax-4 spectrofluorometer (Horiba Jobin Yvon, France). The ratio
153 I_I/I_{III} was calculated as intensity ratio of the first to the third vibronic bands recorded respectively
154 at 373 and 383 nm. All measurements were done at least in triplicate.

155 **2.5. Stability studies**

156 Stability of PEC-NGs in Milli-Q water and physiological salines (NaCl 0.9% eq. 0.154 mol.L⁻¹
157 and PBS) was evaluated (Dioury et al., 2021). To reach NG suspensions having final salinity of
158 NaCl 0.9% or PBS 1X, 80 μ L NaCl 4 mol.L⁻¹ or 52 μ L PBS 40X was added to 2 mL PEC-NG
159 suspension (C_P variation assumed to be inconsiderable). All samples were then vortexed and left
160 for 30 min before DLS analysis at 25 °C, then stored at 4 or 25 °C for revaluation by DLS after
161 1, 3, 7 and 30 days. pH measurements for certain samples were done using a pH meter (Mettler
162 Toledo, Switzerland).

163 **2.6. Enzymatic degradation studies**

164 NG degradation was studied through particle size evolution in the presence of HAase (Yang et
165 al., 2016). Firstly, HAase 30 and 3 mg.mL⁻¹ solutions were prepared by dissolving HAase in
166 Milli-Q water. 10 μ L of these solutions was then vortexed with 1 mL of PEC-NG suspensions of
167 interest to reach final HAase concentrations of 0.3 or 0.03 mg.mL⁻¹. All samples, including
168 samples without HAase as reference, were then analyzed by DLS at predetermined time points
169 during their incubation at 37 °C.

170 **2.7. Curcumin quantification**

171 Curcumin quantification method was adapted from other studies with some modifications
172 (Gómez-Mascaraque, Sipoli, de La Torre, & López-Rubio, 2017; Sarika & James, 2016).
173 Briefly, 200 mL PEC-NG suspension was vortexed with 20 mL of HCl 1 N to protonate HA and
174 facilitate PEC disintegration (Kayitmazer, Koksall, & Iyilik, 2015). The mixture was then
175 vortexed with 1.1 mL (880 mg) of ethanol for curcumin solubilization. The precipitated polymer
176 was then separated by centrifugation at $3,000 \times g$ for 15 min. The curcumin concentration C in
177 the supernatants ($\mu\text{g}\cdot\text{mL}^{-1}$) was determined by UV-visible spectrophotometer Cary 100 (Agilent
178 Technology, USA) with a standard curve of absorbance at 420 nm (A_{420}) in function of curcumin
179 concentration between 0.05-10 $\mu\text{g}\cdot\text{mL}^{-1}$ in water/HCl 1N/EtOH 10/1/55 v/v ($A_{420} = 0.1407 \times C -$
180 0.0022 with $R^2 = 0.9999$). Curcumin concentrations in the starting PEC-NG suspensions
181 ($C_{\text{CUR/SUS}}$) were accordingly deducted, with densities of PEC-NG suspensions and the
182 supernatant (EtOH/aqueous phase 5/1 v/v or 4/1 m/m) at room temperature being 1 and 0.84
183 $\text{g}\cdot\text{mL}^{-1}$ respectively (Rumble, 2021). The loading capacity (LC) and encapsulation efficiency
184 (EE) were calculated as followed:

$$185 \quad \text{LC} = (C_{\text{CUR/SUS}} - C_{\text{CUR/WATER}})/C_{\text{P}} \times 100 (\%) \quad (\text{Equation 1})$$

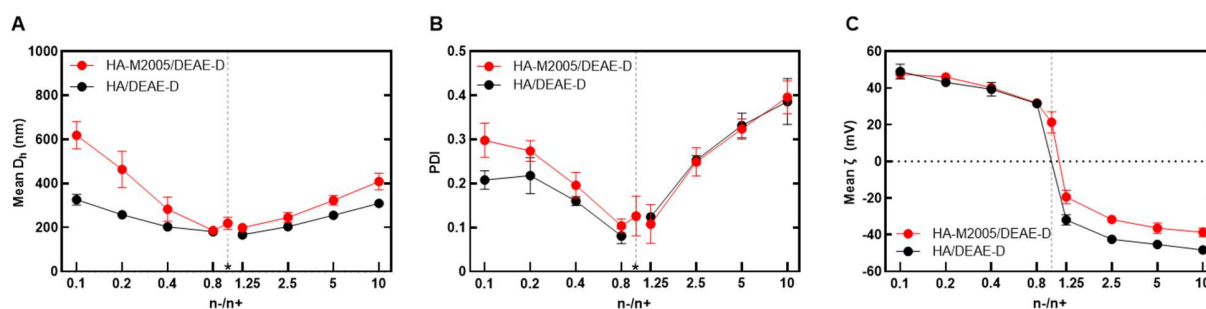
$$186 \quad \text{EE} = (C_{\text{CUR/SUS}} - C_{\text{CUR/WATER}})/C_{\text{CUR0}} \times 100 (\%) \quad (\text{Equation 2})$$

187 with $C_{\text{CUR/WATER}}$ as curcumin concentration of reference sample, which contained solely water
188 saturated in curcumin, C_{P} as polymer concentration and C_{CUR0} as the concentration of added
189 curcumin with respect to the aqueous phase during the preparation.

190 **3. RESULTS AND DISCUSSION**

191 **3.1. PEC-NG initial characterization**

192 PEC-NGs were generated by simply mixing polyanion with polycation solutions, which was
193 spontaneous *via* electrostatic interactions since no chemical reaction was observed from their
194 FT-IR spectra (**Figure S3**). Such preparation process is thus simple and rapid, requiring no
195 organic solvent, chemical agent or high energy. For clarifying the effect of M2005 grafting,
196 **Figure 2** shows particle properties of HA-M2005/DEAE-D PEC-NGs at $C_P = 0.5 \text{ g.L}^{-1}$ after 30
197 min of complexation, compared to those of HA/DEAE-D PEC-NGs from our previous study (Le
198 et al., 2021).

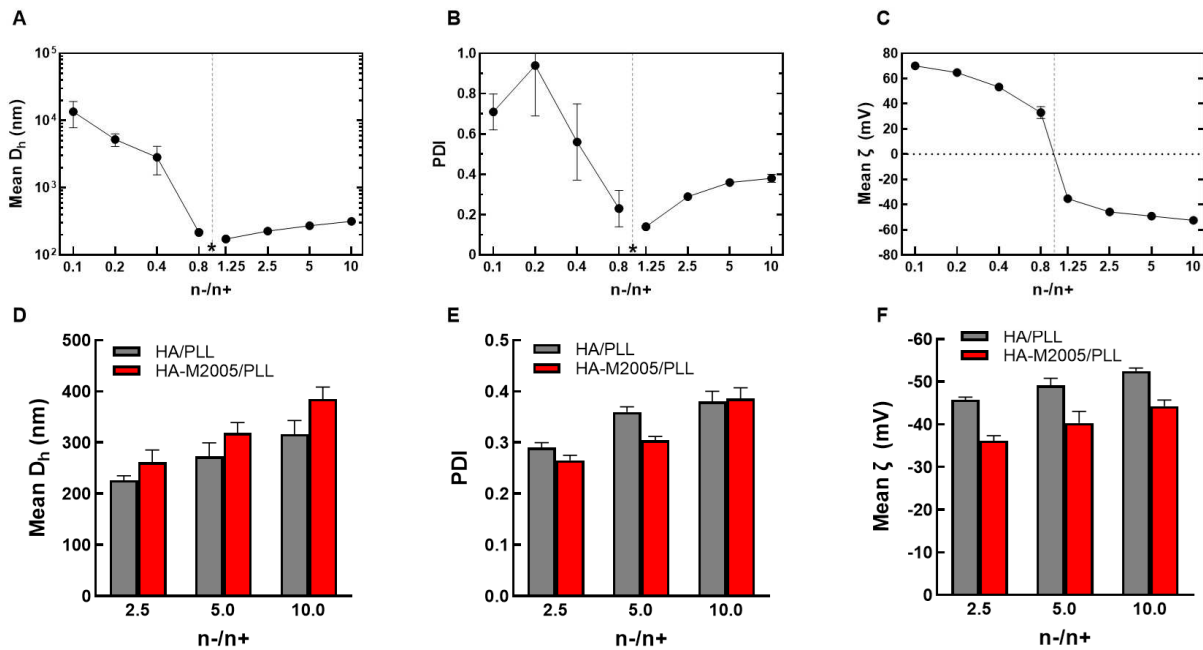


199 **Figure 2.** Mean D_h (A), PDI (B) and mean ζ (C) measured at 25 °C of HA/DEAE-D and HA-
200 M2005/DEAE-D PEC-NGs ($C_P = 0.5 \text{ g.L}^{-1}$ in Milli-Q water) after 30 min of complexation.
201 Asterisk represents $n-/n+ = 1$, at which precipitation was observed for HA/DEAE-D PEC-NGs.
202 Data are presented as mean \pm standard deviation ($n \geq 3$).
203

204 As seen from **Figure 2A-B**, homogeneous HA-M2005/DEAE-D PEC-NGs samples have mean
205 D_h of 200-600 nm and PDI of 0.1-0.4. However, such D_h is always larger than that of
206 HA/DEAE-D PEC-NGs at the same n-/n+ (**Figure 2A**). This may stem from steric effects of the
207 bulky M2005 grafts inside PEC-NGs. It should also be noticed that for the same n-/n+, the mass

208 ratio of polyanion to polycation in HA-M2005/DEAE-D PECs was higher than in HA/DEAE-D
209 PECs to compensate the loss of negative charges after M2005 grafting, which may also
210 contribute to the difference in their particle sizes. Furthermore, the difference in D_h and PDI
211 between the two kinds of PEC-NGs is more obvious at $n-/n+ < 0.8$, where DEAE-D exceeds HA
212 (**Figure 2A-B**). As discussed in our previous work, at $n-/n+ < 0.8$, PECs from intermediate
213 molecular weight HA and high molecular weight DEAE-D showed rapid aggregation continuing
214 after 30 min of complexation, being ascribed to hydrophobic segregation of unstable short
215 double-stranded PEC segments (Le et al., 2021). With M2005 grafts, this effect may be enhanced
216 due to higher hydrophobicity of such segments and hence generate much larger secondary PECs.
217 Regarding net surface charge, HA-M2005/DEAE-D and HA/DEAE-D PEC-NGs show quite a
218 similar curve of mean ζ in function of $n-/n+$ (**Figure 2C**), except the less negative ζ observed at
219 $n-/n+ \geq 1$ for PECs possessing M2005 grafts. This could be attributed to shrinkage of HA
220 backbone towards particle interior due to hydrophobic interactions of M2005 on HA and
221 therefore its negative charges are less accessible on NG surface. Mean ζ of PECs of $n-/n+ = 1$ is
222 hence deviated away from zero when HA-M2005 replaces HA (**Figure 2C**), rendering
223 precipitation absent at stoichiometric $n-/n+$ as observed but assumedly present between $n-/n+$ of
224 1 and 1.25.

225 For preparing HA/PLL PEC-NGs, we also used intermediate molecular weight HA with PLL of
226 higher molecular weight. Such PEC-NGs also present physicochemical parameters (**Figure**
227 **3A-C**) following the same trends in function of $n-/n+$ as HA/DEAE-D PEC-NGs (**Figure 2A-C**).



228

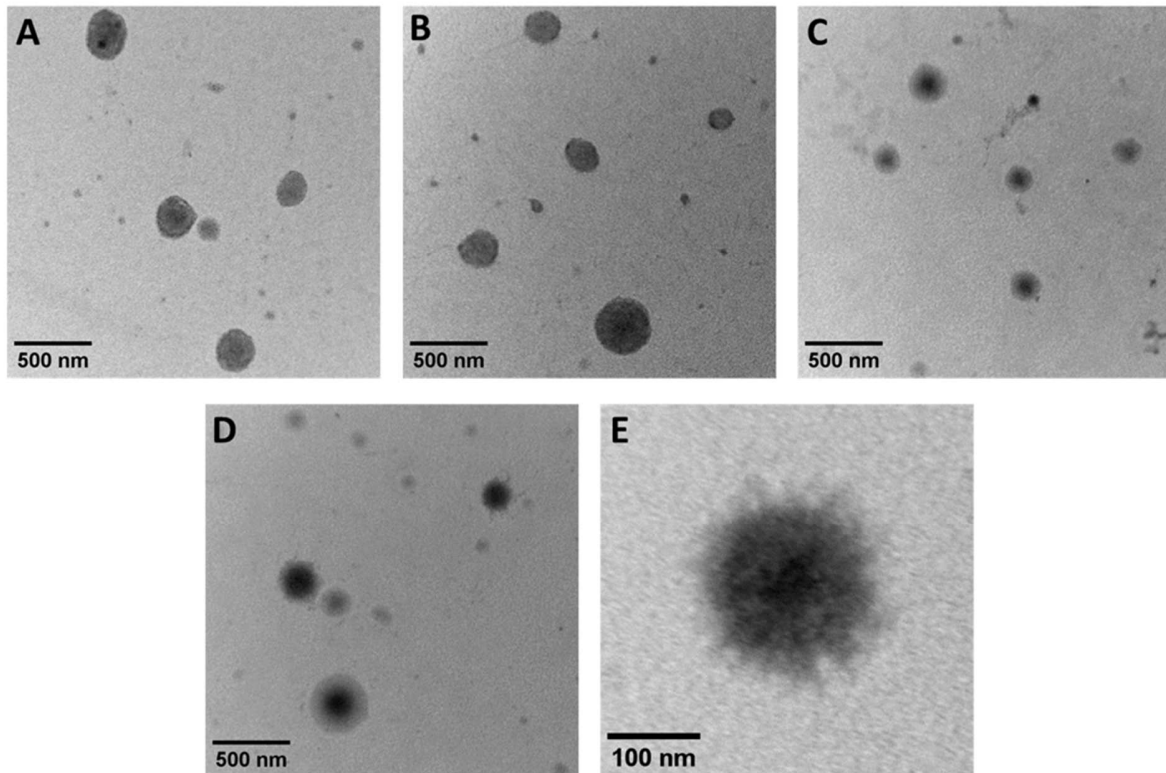
229 **Figure 3.** Mean D_h , PDI and mean ζ of HA/PLL PEC-NGs (A-C respectively) and of HA-
 230 M2005/PLL PEC-NGs in comparison with HA/PLL PEC-NGs (D-F respectively) at $C_p = 0.5$
 231 $g \cdot L^{-1}$ in Milli-Q water after 30 min of complexation. Asterisk represents precipitation at
 232 $n-/n+ = 1$ (DLS not performed). Data are presented as mean \pm standard deviation ($n \geq 3$).

233 HA/PLL PEC-NGs at $n-/n+ > 1$ exhibited consistent characteristics with mean D_h between
 234 100-300 nm and PDI < 0.4 . In contrast, at $n-/n+ < 0.8$, unusually large D_h (1000-10,000 nm) and
 235 PDI (higher than 0.5) were remarked (**Figure 3A-B**). These results approach the upper limit of
 236 reliability for DLS and should not be considered as accurate characteristics but rather a relative
 237 indication of large aggregates uncontrolled in size. PEC-NGs at $n-/n+$ of 0.8, despite their more
 238 relevant D_h (around 200 nm), still showed low batch-to-batch consistency in PDI (**Figure 3B**).
 239 Large aggregates were also reported for HA/PLL PECs of $n-/n+ < 1$ with increasing particle size
 240 over time, from 400 to 800-1000 nm after 8 h (Pan et al., 2019). Such aggregation is probably
 241 caused by stronger intercomplex hydrophobic interactions between PECs containing mainly

242 PLL, which has been known to be considerably hydrophobic upon charge neutralization due to
243 the four succeeding methylene groups in lysine units (Dyson, Wright, & Scheraga, 2006; Pan et
244 al., 2019).

245 Considering the results of HA/PLL PEC-NGs, for HA-M2005/PLL PEC-NGs, we focused only
246 on $n-/n+ > 1$ due to their more consistent and measurable properties. However, for $n-/n+$ of 1.25,
247 precipitation was observed and DLS characterization was not performed. For the other $n-/n+$,
248 M2005 grafts seem to display the same impact as in HA/DEAE-D PECs (**Figure 3D-F** vs.
249 **Figure 2A-C**), i.e. increasing D_h and reducing ζ . Accordingly, this may explain the observed
250 precipitation at $n-/n+$ of 1.25 since the readily low net surface charge at such $n-/n+$ can be further
251 reduced and thus facilitate aggregation.

252 For further characterization of PEC-NGs, the morphologies of all the four types of PEC-NGs at
253 $n-/n+ = 2.5$ and $C_p = 0.5 \text{ g.L}^{-1}$ were also examined by TEM (**Figure 4**), which verified the
254 formation of PEC-NGs as particles having generally spherical shape and particle size in
255 coherence with DLS results. Particle morphologies seem to be distinct depending on the
256 constituent polycation, while M2005 grafts led to no visible difference in this aspect. At higher
257 magnification, some particles can clearly show their structure comprising a dense core
258 surrounded by a corona shell (**Figure 4E**), which confirms the suggested core-shell structure of
259 PEC-NGs.

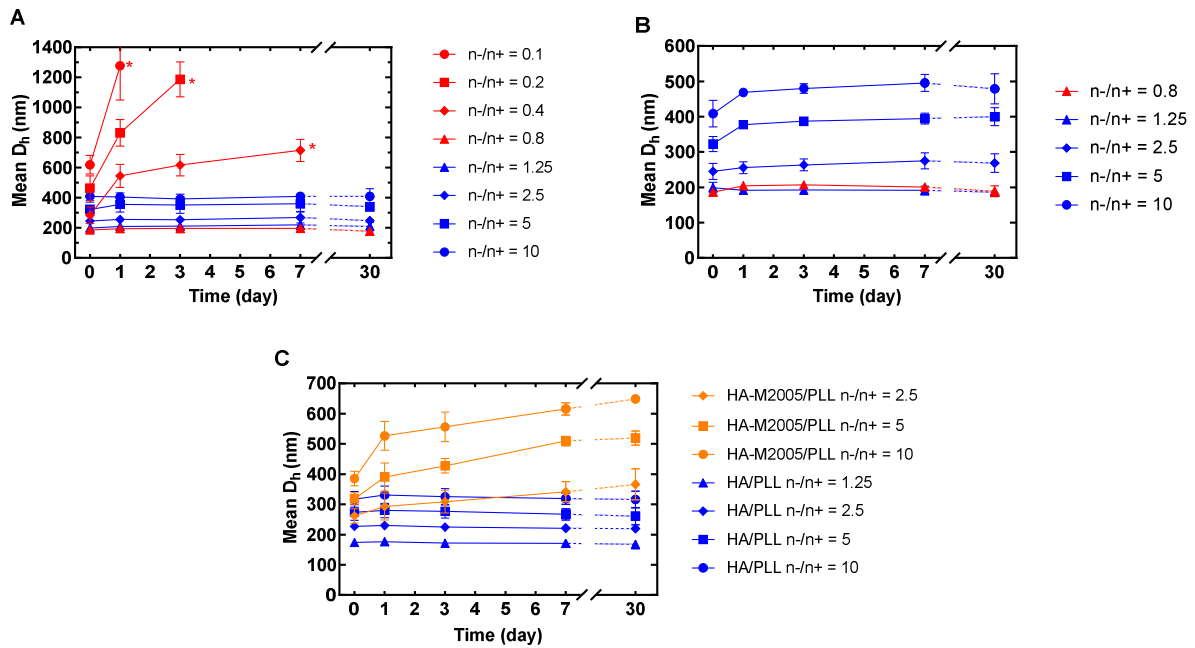


260

261 **Figure 4.** TEM images of PEC-NGs from HA/DEAE-D (A), HA-M2005/DEAE-D (B), HA/PLL
 262 (C and E) and HA-M2005/PLL (D) at $n^-/n^+ = 2.5$ and $C_p = 0.5 \text{ g.L}^{-1}$.

263 3.2. Stability studies

264 Particle sizes of different PEC-NGs at $C_p = 0.5 \text{ g.L}^{-1}$ were monitored during one month in
 265 different conditions (i.e. storage temperature, saline and buffered media) to evaluate the
 266 influence of M2005 grafts and polycation nature on their stability. Stability of mean D_h is shown
 267 in **Figure 5** and their PDIs with the same trend can be consulted from **Figure S4**.



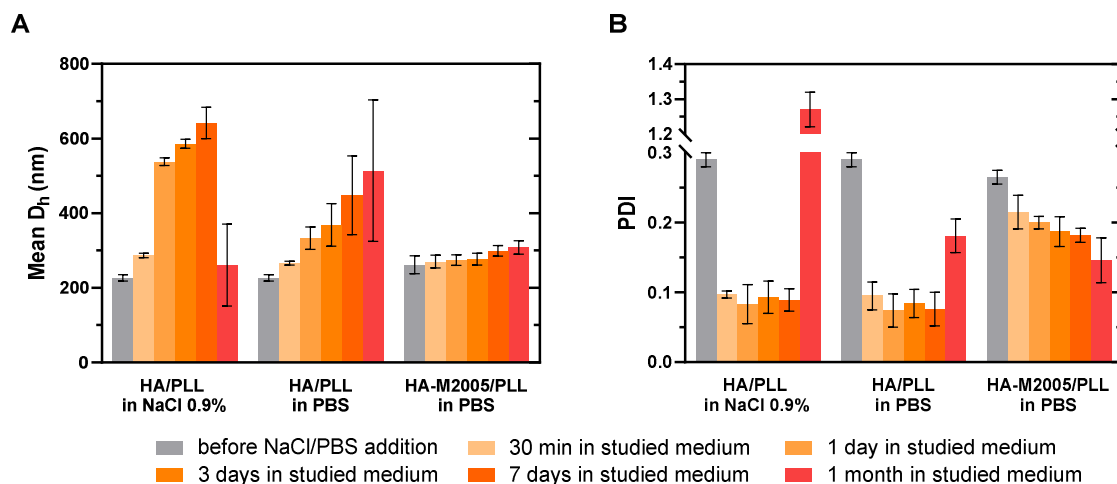
268

269 **Figure 5.** Mean D_h of PEC-NGs (C_P = 0.5 g.L⁻¹ in Milli-Q water) as a function of time: (A) HA-
 270 M2005/DEAE-D PEC-NGs stored at 4 °C, (B) HA-M2005/DEAE-D PEC-NGs stored at 25 °C,
 271 (C) HA-M2005/PLL and HA/PLL PEC-NGs stored at 4 °C. Data are presented as mean ±
 272 standard deviation (n ≥ 3). Asterisks represent samples having large particle sizes (mean D_h >
 273 700 nm) with inconsistently large distribution.

274 As shown in **Figure 5A**, when stored at 4 °C, HA-M2005/DEAE-D PEC-NGs of n-/n+ ≥ 0.8
 275 were stable but those of n-/n+ < 0.8 showed particle size increased after one day. Stability
 276 evaluations were ceased when their mean particle sizes became too high (over 700 nm) with
 277 largely varying PDIs. This is similar to HA/DEAE-D PEC-NGs in our previous work and could
 278 be explained by the same hypothetical mechanism, that neutral double-stranded segments in
 279 these PECs would be very short and hence unstable, favoring their segregation over time to reach
 280 a more stable state (Le et al., 2021).

281 In a second time, HA-M2005/DEAE-D PEC-NGs having good stability at 4 °C were subjected to
282 stability evaluation at 25 °C. Interestingly, higher storage temperature seems to render such
283 PEC-NGs less stable, evidenced by increasing D_h at $n-/n+ \geq 2.5$ (**Figure 5B**). This was not
284 observed with PEC-NGs without M2005 (Le et al., 2021) and therefore can be interpreted as
285 particle aggregation due to enhanced hydrophobic interactions between M2005 grafts on PEC-
286 NG surfaces at higher temperature. Meanwhile, HA-M2005/PLL PEC-NGs at the same $n-/n+$
287 showed D_h increasing over time despite being stored at low temperature (4 °C), in contrast to
288 HA/PLL PEC-NGs which were stable (**Figure 5C**). This suggests that replacing DEAE-D with
289 PLL renders PEC-NGs containing M2005 more susceptible to agglomeration, probably because
290 of stronger interparticle hydrophobic interactions contributed by PLL as mentioned in **Section**
291 **3.1** beside that of M2005.

292 In order to study the stability of PEC-NGs against physiological saline conditions, different PEC-
293 NG formulations were subjected to saline solutions (NaCl 0.9 % and PBS) and stored at 4 °C for
294 stability monitoring. However, the suspensions of HA/DEAE and HA-M2005/DEAE-D
295 PEC-NGs ($C_p = 0.5 \text{ g.L}^{-1}$) showed precipitation after 30 min in NaCl 0.9 % or PBS (results not
296 shown) and were thus not suitable for DLS analysis. This is in accordance with the low stability
297 of HA/DEAE-D PECs upon increasing ionic strength in our previous work (Le et al., 2021) and
298 confirms that such PECs are still highly sensitive to ionic strength even with M20005 grafts.
299 Interestingly, replacing DEAE-D with PLL led to very different behaviors of PECs, which
300 displayed no precipitation and therefore satisfactory for DLS characterization (**Figure 6**).



301
 302 **Figure 6.** (A) Mean D_h and (B) PDI of different PEC-NGs ($C_p = 0.5 \text{ g.L}^{-1}$) stored at $4 \text{ }^\circ\text{C}$ in
 303 different media. Data are presented as mean \pm standard deviation ($n \geq 3$).

304 Following NaCl or PBS addition, HA/PLL PEC-NGs showed significantly increased D_h with an
 305 abrupt fall in PDI. This is most probably due to particle aggregation when electrostatic repulsion
 306 between particles is weakened by counterions through charge screening. As PDI represents the
 307 relation between distribution width and mean value of particle size, the fall of PDI during the
 308 aggregation can be interpreted as the absolute distribution width remaining the same or changing
 309 to a lesser extent than the increase of the mean particle size.

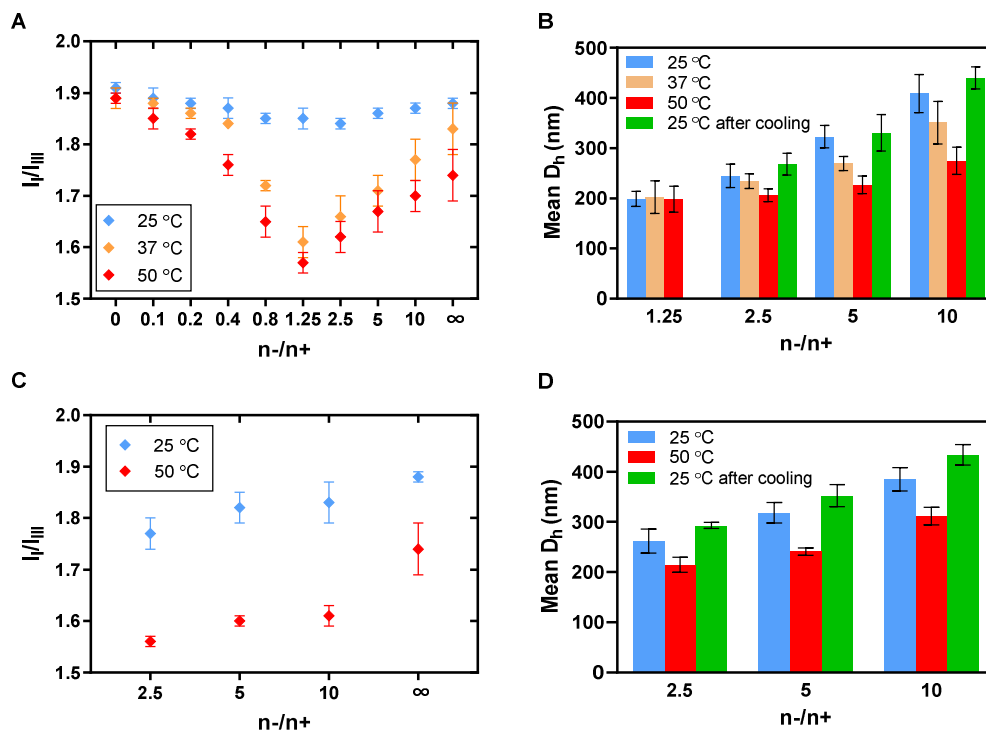
310 Nevertheless, in NaCl 0.9 %, the D_h continued to increase after seven days but decreased after
 311 one month, coinciding with a significant increase in PDI to more than 1. This can be explained
 312 by the appearance of another particle population having lower size of around 10-100 nm (**Figure**
 313 **S5**). As discussed in our previous work (Le et al., 2021), charge screening by salt ions can take
 314 place not only at particle level to cause particle aggregation but also at macromolecular level,
 315 which may cause PEC decomplexation into smaller fragments. In the current case, the latter
 316 effect seems to take place much later than the former. This could be explained by a longer time
 317 required for infiltration of salt ions into the interior of PEC-NGs to interfere with ion pairing.

318 This was also the case in PBS, as shown by the increase in PDI after one month, but seemingly
319 to a lesser extent than in NaCl 0.9 % since the mean particle size did not obviously decrease.
320 Such difference could hardly be explained by the difference between their initial pH, which were
321 measured as 6.28 ± 0.18 and 7.40 ± 0.04 in NaCl 0.9 % and PBS respectively and thus cause no
322 considerable difference in ionization rate and actual n-/n+ of PECs (Supplementary Information
323 **SI-3**). Such a better stability of PEC-NGs in PBS may be due to the long-term pH stability in this
324 buffer. More interestingly, HA-M2005/PLL PEC-NGs showed relatively stable particle size after
325 PBS addition (**Figure 6A**). However, a minor increase in particle size over one month was still
326 observed but to a smaller extent than in Milli-Q water at the same condition (**Figure 5C**) and
327 their PDI was gradually decreased over time. Such results evidence that the presence of salt does
328 not deteriorate but indeed improve the stability of PEC-NGs having M2005 grafts. This finding
329 is especially interesting since PECs from polyelectrolytes disposing weak charges are generally
330 known to be highly unstable under physiological ionic strength (Wu & Delair, 2015). The exact
331 mechanism of such stabilizing effect remains unclear but may be related to salting-out effect of
332 salt, which can reinforce intraparticle hydrophobic interactions between PPO blocks of M2005
333 grafts (Dulong et al., 2012; Gupta et al., 2015; Niang et al., 2016) and therefore stabilize PEC
334 structure.

335 Collectively, such results prove that PEC-NGs with PLL as polycation are more resistant against
336 ionic strength than with DEAE-D. As an explanation, regular charge distribution on both PLL
337 and HA (**Figure 1**) may contribute to more close-knit ion pairing and hence their stronger
338 association. On the contrary, arbitrary distribution of positive charges on DEAE-D may lead to
339 nonoptimal charge compensation with HA and thus more loosely and unstable structure of PECs.

340 **3.3. Thermoresponsiveness studies**

341 Thermoresponsive properties of nanocarriers possessing LCST pendant groups, i.e. shrinkage
342 and increase in hydrophobicity at higher temperature, have been known to be the mechanism and
343 hence the prerequisite for their interesting drug delivery applications, namely triggering and/or
344 controlling the drug release spatiotemporally *in vivo* by applying local hyperthermia (Molina et
345 al., 2015). To verify the thermoresponsiveness of PEC-NGs from HA-M2005, we evaluated at
346 different temperatures their hydrophobicity by fluorescence spectroscopy with pyrene probe and
347 their particle sizes by DLS. The principle of the former technique is that a decrease in intensity
348 ratio of the first to the third peaks (I_I/I_{III}) in the emission spectra upon excitation at 335 nm of
349 pyrene incorporated in the systems indicates the presence of more hydrophobic nanodomains
350 (Burdíková, Mravec, & Pekař, 2016). Compared to previous I_I/I_{III} results of HA/DEAE-D PEC-
351 NGs incorporating pyrene (HA/DEAE-D/Py) (Le et al., 2021), those of HA-M2005/DEAE-D/Py
352 PEC-NGs suggest that M2005 grafts do not significantly enhance the hydrophobicity of PEC-
353 NGs at 25 °C (**Figure S6A**). However, whereas the former system showed unchanged I_I/I_{III} upon
354 heating (**Figure S6B**), HA-M2005/DEAE-D/Py PEC-NGs exhibited lower I_I/I_{III} when the
355 temperature was increased from 25 °C to 37 °C and 50 °C, more significantly at $n-/n+ > 1$ than at
356 $n-/n+ < 1$ (**Figure 7A**). These results prove an increase in hydrophobicity upon heating, probably
357 due to stronger hydrophobic association of the thermosensitive M2005 grafts. This tendency was
358 the same for HA-M2005/PLL/Py PEC-NGs (**Figure 7C**). Furthermore, this effect seems to be
359 more important when $n-/n+$ is nearer to 1 regardless of component polycation (**Figure 7A** and
360 **C**). This may be attributed to PEC structure being readily more compact at such $n-/n+$ (Le et al.,
361 2021), rendering M2005 chains already located in close proximity and hence favoring their
362 approximation to form more hydrophobic clusters.



363
 364 **Figure 7.** I_p/I_{III} in pyrene fluorescence and particle sizes at different temperatures of HA-
 365 M2005/DEAE-D PEC-NGs (A-B respectively) and HA-M2005/PLL PEC-NGs (C-D
 366 respectively) in Milli-Q water. $C_P = 0.5 \text{ g.L}^{-1}$ for particle size analyses and 0.25 g.L^{-1} for pyrene
 367 fluorescence studies due to dilution. The values 0 and ∞ represent solutions containing solely
 368 polycations and polyanions respectively. Data are presented as mean \pm standard deviation ($n \geq$
 369 3).

370 For characterizing the thermal dependence of particle size, we also focused on PEC-NGs with
 371 $n/n+ > 1$ since these systems showed more consistent results of initial particle size (**Section 3.1**).
 372 Upon heating, HA-M2005/DEAE-D PEC-NGs showed a decrease in D_h (**Figure 7B**) and the
 373 same for their PDI (**Figure S7A**). For HA-M2005/PLL PEC-NGs, except for those at $n/n+ =$
 374 1.25 which could not be characterized by DLS because of precipitation (**Section 3.1**), PEC-NGs
 375 at $n/n+ \geq 2.5$ also displayed lower D_h (**Figure 7D**) and PDI (**Figure S7B**) at higher temperature.

376 Such decrease in particle size takes place within only 200-300 s of heating before reaching an
377 equilibrium (**Figure S7D**). In contrast, PECs without M2005 grafts did not show such change
378 upon heating (**Figure S7C**). Together with the earlier results on hydrophobicity, these results
379 suggest that LCST property of M2005 grafts on HA contributes to a quasi-instantaneous series of
380 thermoresponsive behaviors of our PEC-NGs, namely compaction of intraparticle hydrophobic
381 clusters which leads to rapid particle shrinkage. However, different from the increase in
382 hydrophobicity, the shrinkage is less obvious when $n-/n+$ is nearer to 1 and even unobservable at
383 $n-/n+ = 1.25$ for HA-M2005/DEAE-D PEC-NGs, presumably because the readily compact
384 structure of PEC-NGs at $n-/n+$ nearer to 1 is less susceptible to shrinkage than the highly porous
385 structure at other $n-/n+$. Furthermore, after one hour of cooling at room temperature, their D_h
386 resurged but slightly surpassed the initial values (**Figure 7B** and **D**) and less clearly for PDI
387 (**Figure S7A-B**). This suggests a completely reversible thermoresponsive behavior but which
388 may accompany a slight rearrangement within PEC-NG structure. This experiment was repeated
389 up to three cycles of heating-cooling and such reversibility was still conserved during the whole
390 process (**Figure S7E**).

391 **3.4. Curcumin encapsulation**

392 Curcumin was used as a model compound to verify the potential of our system in encapsulating
393 poorly water-soluble drugs. Our previous study reported that pyrene is encapsulated more
394 efficiently in PECs if it is added before the complexation (Le et al., 2021). Thus, the preparation
395 of PEC-NGs encapsulating curcumin in the current work was performed by adding polycation to
396 polyanion solutions readily mixed with curcumin. From pyrene fluorescence studies (**Figure 7**),
397 PEC-NGs having $n-/n+$ of 1.25-2.5 seem to be the most potential for encapsulating hydrophobic
398 molecules. However, our preliminary curcumin encapsulation trials with PEC-NGs of $n-/n+ =$

399 1.25 showed inconsistent results, namely large batch-to-batch variation in visual aspect and
 400 curcumin concentration of the samples (results not shown). This possibly stems from the weak
 401 net surface charge of PEC-NGs at this n-/n+, which facilitate their precipitation and
 402 sedimentation along with the insoluble curcumin in excess. PEC-NGs having n-/n+ of 2.5,
 403 displaying more consistent results (**Table 2**), were thus chosen as the main subjects for these
 404 studies. As shown in **Table 2**, curcumin concentration in HA/DEAE-D/Cur PEC-NGs is higher
 405 than in curcumin-saturated water, proving the encapsulation of curcumin inside such PEC-NGs.
 406 Furthermore, the encapsulation was improved with PEC-NGs having M2005 grafts, most
 407 probably due to M2005 hydrophobic clusters in the NGs.

408 **Table 2.** Curcumin quantification results in different formulations

Formulation parameters		Curcumin quantification results ^c		
System	T _{prep}	C _{CUR} (µg.mL ⁻¹)	LC (%)	EE (%)
Milli-Q/Cur ^a	25 °C	0.30 ± 0.05	-	-
HA/DEAE-D/Cur ^b	25 °C	1.11 ± 0.05	0.16 ± 0.01	0.40 ± 0.03
HA-M2005/DEAE-D/Cur ^b	25 °C	1.70 ± 0.13	0.28 ± 0.03	0.70 ± 0.06
HA/DEAE-D/Cur ^b	50 °C	1.15 ± 0.13	0.17 ± 0.03	0.43 ± 0.06
HA-M2005/DEAE-D/Cur ^b	50 °C	3.55 ± 0.41	0.65 ± 0.08	1.63 ± 0.20
HA-M2005/DEAE-D/Cur ^b	70 °C	3.61 ± 0.18	0.66 ± 0.04	1.65 ± 0.09
HA-M2005/PLL/Cur ^b	50 °C	5.06 ± 0.25	0.94 ± 0.05	2.38 ± 0.12

T_{prep}: preparation temperature, C_{CUR}: curcumin concentration, LC: loading capacity, EE: encapsulation efficiency
^a Milli-Q water saturated in curcumin, ^b C_P= 0.5 g.L⁻¹ and n-/n+ = 2.5, ^c mean ± standard deviation (n ≥ 3)

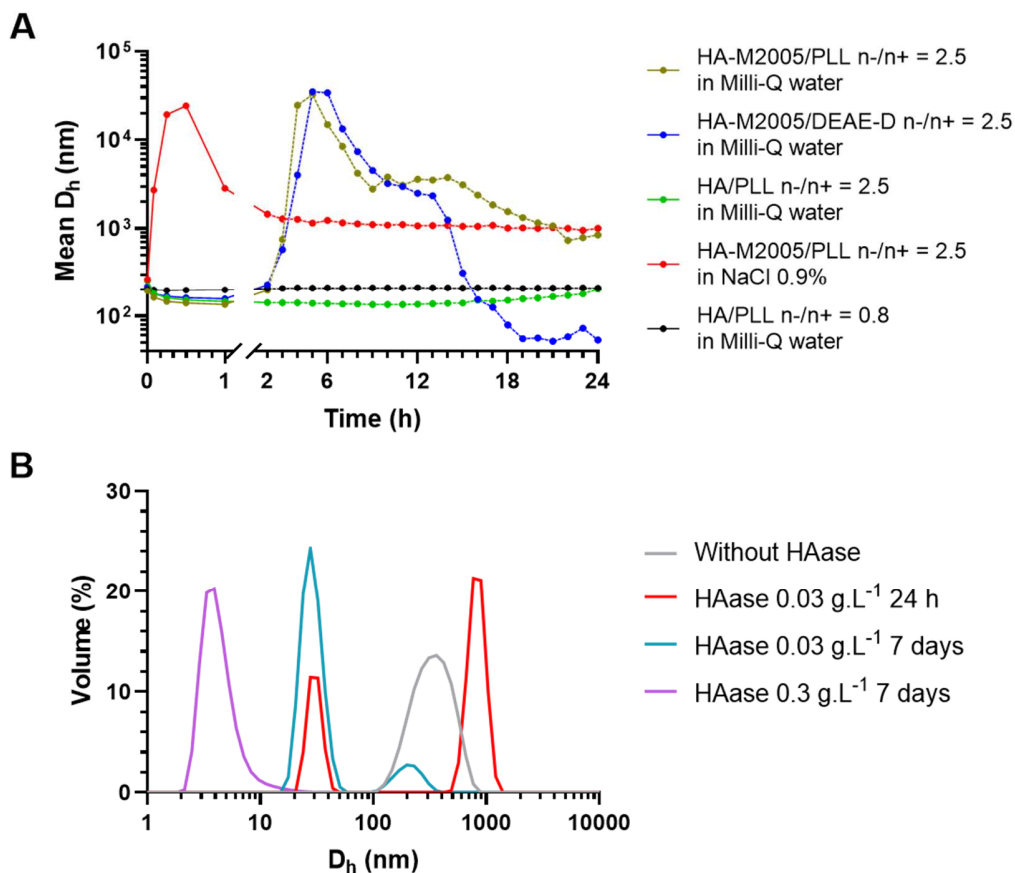
409 To optimize the encapsulation, we carried out the complexation at a higher temperature (50 °C or
 410 70 °C), hypothesizing that this approach would lead to more hydrophobic clusters of M2005 and
 411 incorporate more curcumin, which is then protected from leakage upon cooling by the
 412 hydrophilic shell of PEC-NGs. As expected, HA-M2005/DEAE-D/Cur PEC-NGs prepared at

413 50 °C displayed remarkably higher curcumin content than those prepared at 25 °C, which was
414 not observed for PEC-NGs without M2005 grafts (**Table 2**). This is in coherence with pyrene
415 fluorescence studies and confirms the role of the temperature-dependent hydrophobic
416 interactions of M2005 grafts in encapsulating hydrophobic molecules. However, increasing the
417 complexation temperature from 50 °C to 70 °C did not further improve the encapsulation rate
418 (**Table 2**), suggesting that the hydrophobic interactions of M2005 grafts are already optimal at
419 50 °C. In addition, replacing DEAE-D with PLL also significantly improve the encapsulation
420 (**Table 2**), confirming the more hydrophobic nature of PLL compared with DEAE-D as
421 suggested in **Section 3.1**. Furthermore, PEC-NGs encapsulating curcumin prepared at 50 °C
422 presented comparable mean D_h and ζ (**Table S1**) to those of PEC-NGs without curcumin
423 prepared at room temperature (**Section 3.1**), suggesting that curcumin and the preparation
424 temperature have no considerable effect on ultimate state of PEC-NGs. The modest EE (**Table 2**)
425 may be ascribed to the excessively large amount of starting curcumin during the preparation and
426 the highly hydrophobic nature of this compound with respect to our PEC-NGs which are still
427 globally hydrophilic. Formulation and process optimization is thus still in need before further
428 characterizations like drug release studies or bioassays. Anyway, these results evidence that such
429 PEC-NGs can increase the aqueous solubility of curcumin with possibility of encapsulation
430 tuning and optimization through temperature control, showing therefore the potential for
431 encapsulating other hydrophobic drugs.

432 **3.5. Enzymatic degradation**

433 The current PEC-NGs, as other HA-based nanocarriers, are potential for target drug delivery
434 towards cancer cells since they are supposed to be degraded by HAase overexpressed
435 specifically inside these cells and exhibit therefore more efficient intracellular drug release than

436 in normal cells (Yang et al., 2016). From this perspective, it is of high interest to verify and
 437 understand HAase-induced degradation of our PEC-NGs. To this aim, we investigated the
 438 evolution of their particle size in the presence of HAase 0.03 g.L⁻¹ (12 IU.mL⁻¹) during 24 h at 37
 439 °C. Such evolution of D_h is reported in **Figure 8A**, with PDI following relatively similar trends
 440 in **Figure S8**.



441
 442 **Figure 8.** (A) Temporal evolution of mean D_h of different PEC-NGs in the presence of HAase
 443 0.03 g.L⁻¹ (12 IU.mL⁻¹) during 24 h at 37 °C. (B) Volume-weighted particle size distribution of
 444 HA-M2005/PLL PEC-NGs (n-/n+ = 2.5, C_P = 0.5 g.L⁻¹) in NaCl 0.9% before and after being
 445 treated with HAase at different enzyme concentrations and time points. Data were obtained from
 446 one experiment, results of replicated experiments showed similar trends.

447 Whereas PEC-NGs displayed no significant change in D_h over time in the absence of HAase
448 (results not shown), HA-M2005/PLL and HA-M2005/DEAE-D PEC-NGs of $n-/n+ = 2.5$ in
449 Milli-Q water showed D_h changed after HAase addition, including a decrease in the first one
450 hour followed by a sudden increase to reach a maximum after 5-6 h. For HA/PLL PEC-NGs of
451 the same $n-/n+$, such phenomenon evolved much more slowly as their D_h only started to
452 gradually increase after 12 h of slight diminution since HAase addition (**Figure 8A**) and then
453 showed mean D_h of nearly 2000 nm with PDI of 0.88 after 3 days (results not shown). Such
454 change in particle size may be because HAase preferentially degrades uncomplexed HA on the
455 corona shell of PEC-NGs, leading to reduction of particle size at the beginning but also loss of
456 surface charge and steric effect, which would in turn reduce interparticle electrostatic repulsion
457 and cause hydrophobic aggregation. The speediness of such evolution for PEC-NGs containing
458 M2005 probably stems from their weaker net surface charge and more hydrophobic structure
459 brought about by M2005 grafts (see **Section 3.1**). Meanwhile, HA-M2005/PLL PEC-NGs in
460 NaCl 0.9 % showed an immediate increase in particle size after HAase addition, probably
461 because of two synergistic effects of salt: (i) charge screening to restrict non-specific
462 complexation between HA and HAase, thus enhancing enzyme activity (Astériou, Vincent,
463 Tranchepain, & Deschrevel, 2006) and (ii) reducing electrostatic repulsion between PEC-NGs
464 while reinforcing hydrophobic interactions of M2005 to enhance particle aggregation (see
465 **Section 3.2**). However, after reaching the maxima, the particle sizes started to decrease (**Figure**
466 **8A**), which can be interpreted by PEC deterioration following HA degradation. This was more
467 considerable with DEAE-D than with PLL as polycation, presumably due to the more fragile
468 PEC structure between HA and DEAE-D as described in **Section 3.2**. Meanwhile, HA/PLL PEC-

469 NGs at $n/n+ = 0.8$ presented no change in D_h in the presence of HAase (**Figure 8A**), suggesting
470 a protective effect of PLL shell on HA inside PEC-NGs against the enzyme.

471 Regarding D_h distribution (**Figure 8B**), HA-M2005/PLL PEC-NGs of $n/n+ = 2.5$ treated with
472 HAase 0.03 g.L^{-1} in NaCl 0.9 % over 24 h had a population of low D_h (20-50 nm) beside few
473 large aggregates (500-1000 nm). The former population was further accentuated with
474 disappearance of the aggregates after 7 days, confirming the degradation of PEC-NGs by HAase.
475 For the same treatment time, a higher enzyme concentration of 0.3 g.L^{-1} led to PEC-NGs being
476 broken down into much smaller fragments (2-20 nm). These results further confirm that PEC-NG
477 degradation by HAase is dependent on treatment time and enzyme concentration.

478 **4. CONCLUSION**

479 In this work, mixing the solutions of HA or HA-M2005 with DEAE-D or PLL allowed
480 spontaneous formation of PEC-NGs through electrostatic interactions, which is a rapid and
481 simple elaboration process. M2005 grafts on HA can prompt inter- and intraparticle hydrophobic
482 interactions while also rendering PEC-NGs thermoresponsive, which is applicable in optimizing
483 drug encapsulation. Compared with DEAE-D, PLL can offer additional hydrophobicity and
484 better stabilization of PEC-NGs. A synergistic combination between HA-M2005 and PLL can
485 therefore generate PEC-NGs showing good stability under physiological ionic strength and the
486 highest encapsulation capacity. With HA-M2005 as the main component, these PEC-NGs are not
487 only thermosensitive but also degradable in the presence of HAase, thus promising as a dual-
488 responsive system for targeted delivery of poorly water-soluble drugs. This should be especially
489 advantageous for targeting tumors, where the overexpression of CD44 receptors and HAase
490 should lead to enhanced cellular uptake and degradation of our NGs for drug release, while the
491 thermoresponsiveness of the system may allow controlling not only encapsulation of anticancer

492 drugs, which usually have low aqueous solubility, but also their spatiotemporal delivery *in vivo*
493 by applying local hyperthermia. However, further studies, namely formulation and conservation
494 optimization by freeze-drying and drug release studies, remain to be done before biological *in*
495 *vitro* and *in vivo* evaluations.

496 **ACKNOWLEDGMENTS**

497 We thank the Normandy region and the European Union for their financial support. We also
498 thank Dr Sophie BERNARD and PRIMACEN (the Cell Imaging Platform of Normandy, IRIB,
499 Faculty of Sciences, University of Rouen Normandy; <http://www.primacen.crihan.fr>) for the
500 TEM training session.

501 This paper is dedicated to the memory of our dear colleague Dr Georgeta MOCANU (“Petru
502 Poni” Institute of Macromolecular Chemistry, Iasi, Romania).

503 **REFERENCES**

- 504 Agut, W., Brûlet, A., Taton, D., & Lecommandoux, S. (2007). Thermoresponsive micelles from
505 Jeffamine-b-poly (L-glutamic acid) double hydrophilic block copolymers. *Langmuir*,
506 23(23), 11526-11533. <https://doi.org/10.1021/la701482w>.
- 507 Astériou, T., Vincent, J.-C., Tranchepain, F., & Deschrevel, B. (2006). Inhibition of hyaluronan
508 hydrolysis catalysed by hyaluronidase at high substrate concentration and low ionic
509 strength. *Matrix Biology*, 25(3), 166-174. <https://doi.org/10.1016/j.matbio.2005.11.005>.
- 510 Bonaccorso, A., Carbone, C., Tomasello, B., Italiani, P., Musumeci, T., Puglisi, G., et al. (2021).
511 Optimization of dextran sulfate/poly-l-lysine based nanogels polyelectrolyte complex for
512 intranasal ovalbumin delivery. *Journal of Drug Delivery Science and Technology*, 65,
513 102678. <https://doi.org/10.1016/j.jddst.2021.102678>.

- 514 Bordat, A., Boissenot, T., Nicolas, J., & Tsapis, N. (2019). Thermoresponsive polymer
515 nanocarriers for biomedical applications. *Advanced Drug Delivery Reviews*, 138, 167-
516 192. <https://doi.org/10.1016/j.addr.2018.10.005>.
- 517 Burdíková, J., Mravec, F., & Pekař, M. (2016). The formation of mixed micelles of sugar
518 surfactants and phospholipids and their interactions with hyaluronan. *Colloid and
519 Polymer Science*, 294(5), 823-831. <https://doi.org/10.1007/s00396-016-3840-8>.
- 520 Debele, T. A., Mekuria, S. L., & Tsai, H.-C. (2016). Polysaccharide based nanogels in the drug
521 delivery system: Application as the carrier of pharmaceutical agents. *Materials Science
522 and Engineering: C*, 68, 964-981. <https://doi.org/10.1016/j.msec.2016.05.121>.
- 523 Díaz-Montes, E. (2021). Dextran: Sources, Structures, and Properties. *Polysaccharides*, 2(3),
524 554-565. <https://doi.org/10.3390/polysaccharides2030033>.
- 525 Dioury, F., Callewaert, M., Cadiou, C., Henoumont, C., Molinari, M., Laurent, S., et al. (2021).
526 Pyclyen-based Gd complex with ionisable side-chain as a contrastophore for the design of
527 hypersensitive MRI nanoprobe: Synthesis and relaxation studies. *Results in Chemistry*,
528 3, 100237. <https://doi.org/10.1016/j.rechem.2021.100237>.
- 529 Dulong, V., Mocanu, G., Picton, L., & Le Cerf, D. (2012). Amphiphilic and thermosensitive
530 copolymers based on pullulan and Jeffamine®: Synthesis, characterization and
531 physicochemical properties. *Carbohydrate Polymers*, 87(2), 1522-1531.
532 <https://doi.org/10.1016/j.carbpol.2011.09.049>.
- 533 Dyson, H. J., Wright, P. E., & Scheraga, H. A. (2006). The role of hydrophobic interactions in
534 initiation and propagation of protein folding. *Proceedings of the National Academy of
535 Sciences*, 103(35), 13057-13061. <https://doi.org/10.1073/pnas.0605504103>.

536 Gandhi, A., Paul, A., Sen, S. O., & Sen, K. K. (2015). Studies on thermoresponsive polymers:
537 Phase behaviour, drug delivery and biomedical applications. *Asian Journal of*
538 *Pharmaceutical Sciences*, 10(2), 99-107. <https://doi.org/10.1016/j.ajps.2014.08.010>.

539 Gómez-Mascaraque, L. G., Sipoli, C. C., de La Torre, L. G., & López-Rubio, A. (2017).
540 Microencapsulation structures based on protein-coated liposomes obtained through
541 electrospraying for the stabilization and improved bioaccessibility of curcumin. *Food*
542 *Chemistry*, 233, 343-350. <https://doi.org/10.1016/j.foodchem.2017.04.133>.

543 Graham, S., Marina, P. F., & Blencowe, A. (2019). Thermoresponsive polysaccharides and their
544 thermoreversible physical hydrogel networks. *Carbohydrate Polymers*, 207, 143-159.
545 <https://doi.org/10.1016/j.carbpol.2018.11.053>.

546 Gulick, T. (1997). Transfection using DEAE - dextran. *Current Protocols in Molecular Biology*,
547 40(1), 9.2. 1-9.2. 10. <https://doi.org/10.1002/0471142727.mb0902s40>.

548 Gupta, N. R., Wadgaonkar, P. P., Rajamohanam, P., Ducouret, G., Hourdet, D., Creton, C., et al.
549 (2015). Synthesis and characterization of PEPO grafted carboxymethyl guar and
550 carboxymethyl tamarind as new thermo-associating polymers. *Carbohydrate Polymers*,
551 117, 331-338. <https://doi.org/10.1016/j.carbpol.2014.09.073>.

552 Huguet, M., Neufeld, R., & Dellacherie, E. (1996). Calcium-alginate beads coated with
553 polycationic polymers: comparison of chitosan and DEAE-dextran. *Process*
554 *Biochemistry*, 31(4), 347-353. [https://doi.org/10.1016/0032-9592\(95\)00076-3](https://doi.org/10.1016/0032-9592(95)00076-3).

555 Karimi, M., Sahandi Zangabad, P., Ghasemi, A., Amiri, M., Bahrami, M., Malekzad, H., et al.
556 (2016). Temperature-responsive smart nanocarriers for delivery of therapeutic agents:
557 applications and recent advances. *ACS Applied Materials & Interfaces*, 8(33), 21107-
558 21133. <https://doi.org/10.1021/acsami.6b00371>.

559 Kayitmazer, A., Koksak, A., & Iyilik, E. K. (2015). Complex coacervation of hyaluronic acid and
560 chitosan: effects of pH, ionic strength, charge density, chain length and the charge ratio.
561 *Soft Matter*, 11(44), 8605-8612. <https://doi.org/10.1039/C5SM01829C>.

562 Kim, Y. K., Kim, E.-J., Lim, J. H., Cho, H. K., Hong, W. J., Jeon, H. H., et al. (2019). Dual
563 stimuli-triggered nanogels in response to temperature and pH changes for controlled drug
564 release. *Nanoscale Research Letters*, 14(1), 1-9. <https://doi.org/10.1186/s11671-019-2909-y>.

566 Le, H. V., Dulong, V., Picton, L., & Le Cerf, D. (2021). Polyelectrolyte complexes of hyaluronic
567 acid and diethylaminoethyl dextran: Formation, stability and hydrophobicity. *Colloids
568 and Surfaces A: Physicochemical and Engineering Aspects*, 629, 127485.
569 <https://doi.org/10.1016/j.colsurfa.2021.127485>.

570 Madau, M., Le Cerf, D., Dulong, V., & Picton, L. (2021). Hyaluronic Acid Functionalization
571 with Jeffamine® M2005: A Comparison of the Thermo-Responsiveness Properties of the
572 Hydrogel Obtained through Two Different Synthesis Routes. *Gels*, 7(3), 88.
573 <https://doi.org/10.3390/gels7030088>.

574 Manosroi, A., & Manosroi, J. (1997). Micro encapsulation of human insulin DEAE-dextran
575 complex and the complex in liposomes by the emulsion non-solvent addition method.
576 *Journal of Microencapsulation*, 14(6), 761-768.
577 <https://doi.org/10.3109/02652049709006826>.

578 Molina, M., Asadian-Birjand, M., Balach, J., Bergueiro, J., Miceli, E., & Calderón, M. (2015).
579 Stimuli-responsive nanogel composites and their application in nanomedicine. *Chemical
580 Society Reviews*, 44(17), 6161-6186. <https://doi.org/10.1039/C5CS00199D>.

581 Necas, J., Bartosikova, L., Brauner, P., & Kolar, J. (2008). Hyaluronic acid (hyaluronan): a
582 review. *Veterinární Medicína*, 53(8), 397-411. <https://doi.org/10.17221/1930-VETMED>.

583 Niang, P. M., Huang, Z., Dulong, V., Souguir, Z., Le Cerf, D., & Picton, L. (2016). Thermo-
584 controlled rheology of electro-assembled polyanionic polysaccharide (alginate) and
585 polycationic thermo-sensitive polymers. *Carbohydrate Polymers*, 139, 67-74.
586 <https://doi.org/10.1016/j.carbpol.2015.12.022>.

587 Pan, W., Yin, D.-X., Jing, H.-R., Chang, H.-J., Wen, H., & Liang, D.-H. (2019). Core-Corona
588 structure formed by hyaluronic acid and poly (L-lysine) via kinetic path. *Chinese Journal
589 of Polymer Science*, 37(1), 36-42. <https://doi.org/10.1007/s10118-018-2166-z>.

590 Rumble, J. (2021). CRC Handbook of Chemistry and Physics, 102nd Edition (Internet Version
591 2021). CRC Press: Boca Raton, FL, USA. <https://hcbp.chemnetbase.com>.

592 Sarika, P., & James, N. R. (2016). Polyelectrolyte complex nanoparticles from cationised gelatin
593 and sodium alginate for curcumin delivery. *Carbohydrate Polymers*, 148, 354-361.
594 <https://doi.org/10.1016/j.carbpol.2016.04.073>.

595 Siow, W. X., Chang, Y.-T., Babič, M., Lu, Y.-C., Horák, D., & Ma, Y.-H. (2018). Interaction of
596 poly-L-lysine coating and heparan sulfate proteoglycan on magnetic nanoparticle uptake
597 by tumor cells. *International Journal of Nanomedicine*, 13, 1693.
598 <https://doi.org/10.2147/IJN.S156029>.

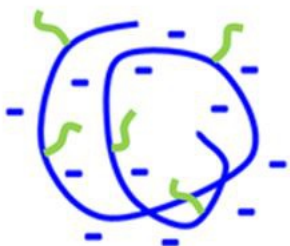
599 Stern, R. (2008). *Hyaluronidases in Cancer Biology*. In R. Stern (Ed.), *Hyaluronan in Cancer
600 Biology* (pp. 207-220). San Diego: Academic Press. [https://doi.org/10.1016/B978-
601 012374178-3.10012-2](https://doi.org/10.1016/B978-012374178-3.10012-2).

602 Wu, D., & Delair, T. (2015). Stabilization of chitosan/hyaluronan colloidal polyelectrolyte
603 complexes in physiological conditions. *Carbohydrate Polymers*, 119, 149-158.
604 <https://doi.org/10.1016/j.carbpol.2014.11.042>.

605 Xu, H., Niu, M., Yuan, X., Wu, K., & Liu, A. (2020). CD44 as a tumor biomarker and
606 therapeutic target. *Experimental Hematology & Oncology*, 9(1), 1-14.
607 <https://doi.org/10.1186/s40164-020-00192-0>.

608 Yang, Y., Zhang, Y.-M., Chen, Y., Chen, J.-T., & Liu, Y. (2016). Polysaccharide-based
609 noncovalent assembly for targeted delivery of taxol. *Scientific Reports*, 6(1), 1-10.
610 <https://doi.org/10.1038/srep19212>.

611



HA-M2005

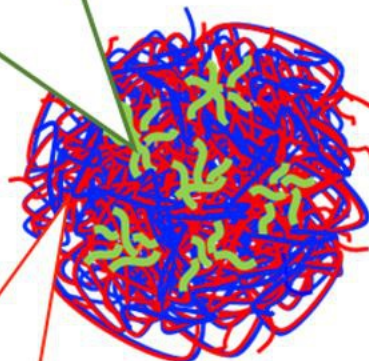
M2005 grafts
[Poly(ethylene oxide)-co-poly(propylene oxide)]
✓ Thermoresponsiveness
↑ Hydrophobicity + NG stability



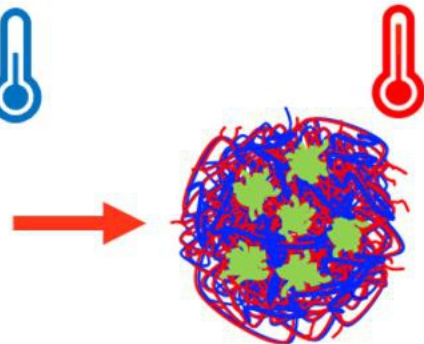
Simple mixing



DEAE-D or PLL



Thermoresponsive
PEC-NGs



Polycation = PLL
↑ Hydrophobicity + NG stability